North American Power Symposium (NAPS), San Luis Obispo, California, October 1999.

Hopf Bifurcation Control in Power Systems Using Power System Stabilizers and Static Var Compensators

N. Mithulananthan Claudio A. Cañizares John Reeve
University of Waterloo
Department of Electrical & Computer Engineering
Waterloo, ON, Canada N2L 3G1
c.canizares@ece.uwaterloo.ca

***Abstract*—This paper compares the use of Power System Stabilizers (PSS) and Static Var Compensators (SVC) to damp power/frequency oscillations in power systems. These oscillations are first shown to be associated with Hopf bifurcations. Then, bifurcation theory is used to analyze the phenomena and design corrective measures. The effect on the bifurcation critical eigenvalues, and hence on the power/frequency oscillations, of the gains of the PSS and the SVC controls is also studied on a 16-bus test system. Finally, time domain simulations are used to compare the effectiveness of these controllers on damping oscillations on the test network.**

Keywords: Power oscillation control, Hopf bifurcations, PSS, SVC.

I. Introduction

Power/frequency oscillatory phenomena in power systems have been typically analyzed using eigenvalue computations, and solved by adding Power System Stabilizers (PSS) to generators [1]. However, given the characteristics of this problem, alternative analysis techniques can be developed using bifurcation theory [2]. Furthermore, with the more recent development of Flexible AC Transmission System (FACTS) controllers [3], such as the Static var Compensator (SVC), there have been a number of studies for the use of these controllers in power/frequency oscillation control [2, 4].

This paper first presents bifurcation theory to study the power/frequency oscillation problem, and then compares PSS versus SVC controllers as solutions to the oscillatory problem in a test system.

A. Bifurcations

Saddle-node and Hopf bifurcations have been identified as some of the reasons behind instabilities in power systems [5]. Saddle-node bifurcations basically consist of loss of system equilibrium, and have been associated, together with limit-induced bifurcations that also result on loss of equilibrium due to limits, with voltage collapse problems [6]. Hopf bifurcations, on the other hand, produce limit cycles, leading to oscillatory instabilities; these types of bifurcations have been detected in a variety of power system models [5, 7, 8, 9].

Hopf bifurcations arise from voltage control issues, such as fast acting automatic voltage regulators in generators [8], and are usually triggered by contingencies in the system. In most cases, these bifurcations heavily loaded systems operating close the "tip of the nose curve", where the region of attraction of the operating point becomes very small [10]; hence, the system is not able to withstand perturbations. This is very relevant for present power systems operating near their stability limits due to economical and environmental constraints. Examples of Hopf bifurcation induced system collapses occurred in Sri Lanka on May 2, 1995 [11], and in the Western System Coordination Council (WSCC) system on August 10, 1996. The consequences were severe, e.g., in the WSCC system, reports indicate that approximately 7.5 million customers were interrupted from continuous supply, whereas in the Sri Lanka event, it took about an hour to bring the system back to normal, with a system wide outage lasting more than 30 minutes.

B. Power/Frequency Oscillation Damping

Of the wide range of power system controllers available or being considered as effective devices for damping oscillations, the most widely known and used on the generator side is the PSS. More recently, FACTS controllers (e.g., SVC) have been proposed and used for oscillation damping purposes. The main advantage of these controllers is that they can be designed to use suitable control signals and placed at locations on the transmission system to achieve the best possible damping. In [2], the authors study the control of Hopf bifurcations by means of an SVC on a generator-infinite bus test system and on a three machine test system, by placing the SVC between two generators. Coordinated tuning of PSSs and FACTS controllers is also another way of providing the desirable level of damping.

In the current paper, the ability of PSS and SVC controllers for removing Hopf bifurcations is analyzed and compared. The effect of the PSS and SVC controller gains on the critical eigenvalue is also studied, to determine how sensitive power/frequency oscillations are to these controllers. Simulations are carried out on an approximated model of a 16-bus power system proposed in [12]. The placement of a PSS relied on a classical participation factor analysis [1], whereas the placement of an SVC was done based on the voltage collapse concept of the weakest bus in a power system [13, 14].

This paper is organized as follows: Section II introduces the basic theory behind Hopf bifurcations and power system state matrices and their associated eigenvalues. Basic operation of PSS and SVC controllers are given in Section III, together with a brief discussion on PSS and SVC optimal placement. In Section IV, the 16-bus test system is briefly introduced and a detailed discussion on the results obtained from damping power/frequency oscillations using these controllers is presented. Section V summarizes the major contributions made in this paper, and future research directions are discussed.

II. Basic Background

A. Hopf Bifurcations and Power/Frequency Oscillations

Hopf bifurcations are characterized by periodic orbits (limit cycles) emerging around an equilibrium point, and can be determined with the help of linearized analysis, as at these bifurcation points the system Jacobian has a pair of purely imaginary eigenvalues [15].

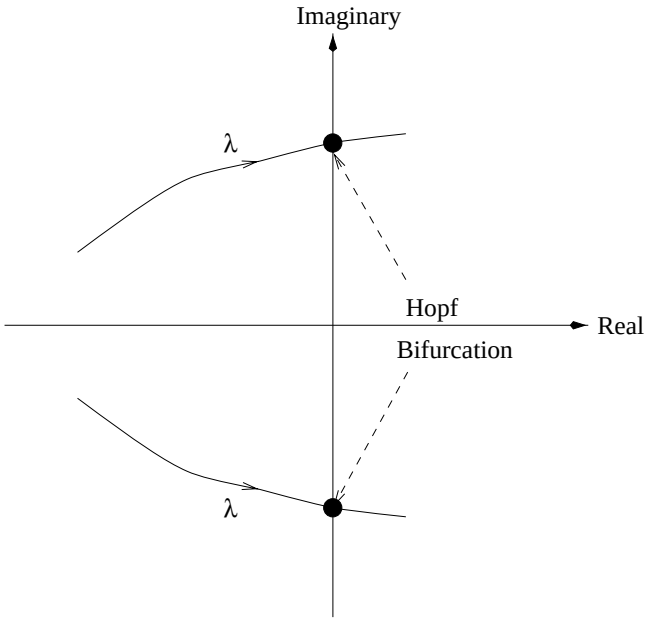

Fig. 1. Locus of the critical eigenvalue on a Hopf bifurcation.

Consider a dynamical system modeled by a set of ordinary differential equations (ODE) as follows:

$$\dot{x} = f(x, \lambda)$$

where x is a n-dimensional state vector and λ is a scalar parameter, i.e., $x \in \Re^n$ and $\lambda \in \Re$. When the parameter λ varies, the equilibrium points x_o for this system, i.e., the state points defined by the solutions of

$$f(x_o, \lambda) = 0 \tag{1}$$

change, and so do the eigenvalues of the corresponding system Jacobian or state matrix evaluated at this equilibrium point, i.e., the eigenvalues of $\partial f/\partial x|_o$.

The equilibrium point defined in state space by (1) is asymptotically stable if all the eigenvalues of the system Jacobian have negative real parts at that point. As the parameter λ changes, the eigenvalues associated with the corresponding equilibrium point change as well. The point where a complex conjugate pair of eigenvalues reach the imaginary axis with changes in λ, say (x_o, λ_o), is known as the Hopf bifurcation point. This phenomenon is illustrated in Fig. 1 by the locus of the "critical" eigenvalues in the complex plane, i.e., the "bifurcating" complex conjugate pair of eigenvalues.

At a Hopf bifurcation point (x_o, λ_o), the following transversality conditions should be satisfied [15]:

1. $f(x_o, \lambda_o) = 0$.
2. The Jacobian matrix evaluated at (x_o, λ_o) should only have a simple pair of purely imaginary eigenvalues, $\mu = \pm j\beta$.
3. The rate of change of the real part of the purely imaginary eigenvalues with respect to the parameter λ should be nonzero, i.e.,

$$\frac{\mathrm{d}\ \mathrm{Re}\{\mu\}}{\mathrm{d}\lambda} \neq 0$$

These conditions basically state that a Hopf bifurcation corresponds to a system equilibrium with a pair of purely imaginary eigenvalues with all other eigenvalues having non-zero real parts, and that the pair of bifurcating or critical eigenvalues cross the imaginary axis with nonzero "speed".

Power/frequency oscillation problems in power networks are basically represented by sustained or growing oscillations of system frequency accompanied by excursions in power low due to a loss of synchronizing torque, i.e., a lack of balance between input mechanical torque and output electrical torque in some generators [1]. This problem has been classically associated with a pair of eigenvalues of system equilibria (operating points) crossing the imaginary axis of the complex plane from the left half-plane to the right half-plane when the system undergoes sudden large changes, which are most commonly produced by system contingencies (e.g., line outages). If this particular oscillatory problem is studied using more gradual changes in the system, such as changes on slow varying parameters like system loading, this phenomenon can be directly viewed as a Hopf bifurcation problem, as suggested in [2]. Thus, in the current paper, Hopf bifurcation theory is used to analyze the appearance of sustained power/frequency oscillations on a test system due to a sudden change in system loading (contingency), and to devise damping techniques based on PSS and SVC controllers, as shown in Section IV.

B. Power System Eigenvalue Analysis

In general, power systems are modeled by the following set of differential and algebraic equations (DEA):

$$\begin{aligned} \dot{x} &= f(x, y, \lambda, p) \\ 0 &= G(x, y, \lambda, p) \end{aligned} \tag{2}$$

where $x \in \Re^n$ is a vector of state variables associate with dynamic states of generators, loads, and other system controllers; $y \in \Re^m$ is a vector of algebraic variables associate with steady-state variables resulting from neglecting fast dynamics, e.g., some load voltage phasor magnitudes and angles, HVDC links, etc.; $\lambda \in \Re^\ell$ is a set of uncontrollable parameters, such as active and reactive power load variations; and $p \in \Re^k$ is a set of controllable parameters such as tap settings, Automatic Voltage Regulator (AVR) and SVC reference voltages.

For the eigenvalue analysis (small signal stability or steady state stability analysis), (2) can be linearized around an equilibrium point (x_o, y_o) for given values of the parameters (λ, p) (an operating point). Thus,

$$\begin{bmatrix} \Delta\dot{x} \\ 0 \end{bmatrix} = \underbrace{\begin{bmatrix} J_1 & J_2 \\ J_3 & J_4 \end{bmatrix}}_{J} \begin{bmatrix} \Delta x \\ \Delta y \end{bmatrix} \tag{3}$$

where, J is the system Jacobian, and $J_1 = \partial f/\partial x|_0$, $J_2 = \partial f/\partial y|_0$, $J_3 = \partial f/\partial x|_0$, $J_4 = \partial f/\partial y|_0$. If it is assumed that J_4 is nonsingular, the system eigenvalues can be readily computed by eliminating the vector of algebraic variable Δy in (3),

$$\Delta\dot{x} = (J_1 - J_2\ J_4^{-1}\ J_3)\Delta x = A\ \Delta x$$

i.e., the DAE system can be reduced to a set of ODE equations [16]. Hence, Hopf bifurcations on power system models are typically detected by monitoring the eigenvalues of matrix A as the system parameters (λ, p) change.

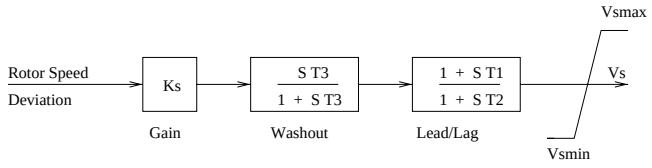

Fig. 2. A typical block diagram of a PSS [1].

III. Basic operation and placement of PSS and SVC Controllers

A. Power System Stabilizer or PSS

As explained in [1], a PSS can be viewed as an additional block of a generator excitation control or AVR, added to improve the overall power system dynamic performance, especially to control power/frequency oscillations. Thus, the PSS uses auxiliary stabilizing signals such as shaft speed, terminal frequency and/or power to change the input signal to the AVR. This is a very effective method of enhancing small-signal stability performance on a power network.

There are three basic blocks in a PSS, as illustrated in the typical block diagram of Fig. 2, namely, the Gain block, the Washout block and the Phase-compensation block. The Phase-compensation block provides the appropriate phase-lead characteristic to compensate for the phase lag between the exciter input and the generator electrical (air-gap) torque; in practice, two or more first-order blocks may be used to achieve the desired phase compensation. The Washout block serves as a high-pass filter, where the time constant T_3 is high enough to allow the signal associated with oscillations in rotor speed to pass unchanged; without the Washout block, the steady state changes would modify the terminal voltages. Finally, the stabilizer Gain block determines the amount of damping introduced by the PSS. In the current paper, a PSS with two Phase-Lead/Lags, a Washout block and a Gain block is used for controlling Hopf bifurcations in the system.

The placement of PSS for control of Hopf bifurcations is decided based on participation factor analysis, which consists of identifying the dominant state variable associated with a particular mode (eigenvalue). One problem with using right and left eigenvectors individually for identifying the relationship between the state and the modes is that the elements of the eigenvectors are dependent on the units and scaling associated with the state variables. This problem can be avoided by combining the right and left eigenvectors associated with each mode; this combined matrix is known as the participation factor matrix and is defined as follows:

$$P = \begin{bmatrix} P_1 & P_2 & \cdots & P_n \end{bmatrix}$$

where

$$P_i = \begin{bmatrix} P_{1i} \\ P_{2i} \\ \vdots \\ P_{ni} \end{bmatrix} = \begin{bmatrix} \phi_{1i}\psi_{i1} \\ \phi_{2i}\psi_{i2} \\ \vdots \\ \phi_{ni}\psi_{in} \end{bmatrix}$$

ϕ_{ki} is the element on the k^{th} row and i^{th} column of the right modal matrix ϕ, i.e., the k^{th} entry of the right eigenvector ϕ_i, and ψ_{ik} is the element on the i^{th} row and k^{th} column of the left modal matrix ψ, i.e., the k^{th} entry of the left eigenvector ψ_i. Since ϕ_{ki} measures the activity of the k^{th} state variable in the i^{th} mode, and ψ_{ik} weighs the contribution of this activity to the mode, the product P_{ki} measures the net participation. By multiplying the elements of the left and right eigenvectors, the participation factor is dimensionless; thus, the sum of the participation factors associated with any mode or with any state variable is equal to one.

In this paper, the PSS was placed at the generator bus whose state variables are dominant in the Hopf bifurcation mode, i.e., the generator bus with the largest participation factor associated with the purely imaginary complex pair of eigenvalues at the bifurcation.

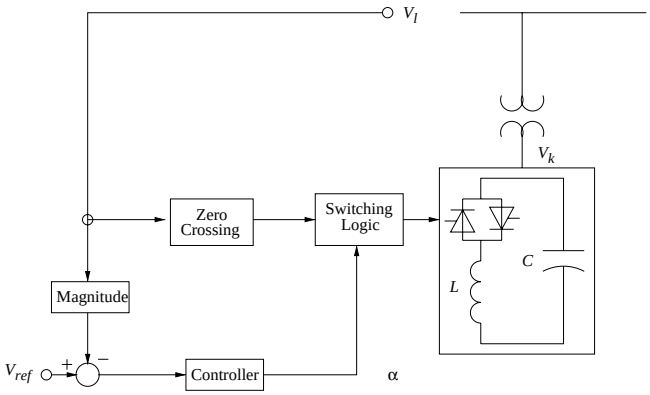

Fig. 3. Basic SVC structure.

B. Static var Compensator

As explained in [17], an SVC is a shunt connected static var generator/absorber whose output is adjusted to exchange capacitive or inductive current so as to maintain or control specific variables. Typically the controlled variable is the SVC bus voltage. SVCs were first developed in the late 1960s for the compensation of large fluctuating industrial loads, such as electric arc furnaces. These kinds of compensators used either thyristor-switched capacitors (TSC) or a thyristor-controlled reactor (TCR) with fixed, permanently connected, power factor correcting capacitors. By the late 1970s it became evident that dynamic compensation was needed to achieve better utilization of existing generation and transmission facilities. Thus, SVCs using TCRs in combination with TSCs and fixed capacitive filters on the secondary side of a coupling transformer were develop to provide voltage support, resulting in increased transient stability margins and improved system damping.

The most popular configurations of the SVC controllers are the fixed capacitor (FC) with a TCR, and the TSC with TCR. A simplified diagram of an SVC with FC and TCR together with its basic control structure is shown in Fig. 3. In Fig. 4, the basic steady-state bus voltage control strategy used in most SVCs is depicted; the sharp corners on the graph correspond to the limits of the TCR, i.e., when the TCR is fully on (inductive) and when is fully off (capacitive).

The selected dynamic analysis tools permit the controller to be modeled as a User Defined SVC (UDSVC) [18, 19]. The UDSVC used here consists of a static Gain block with limits, two Lead/Lag blocks with limits, and an end block (SD-2) as shown in Fig. 5. The SD-2 end block is a static device that represents the TCR and FC as an equivalent, nonlinear, controllable susceptance B_{SVC} [18].

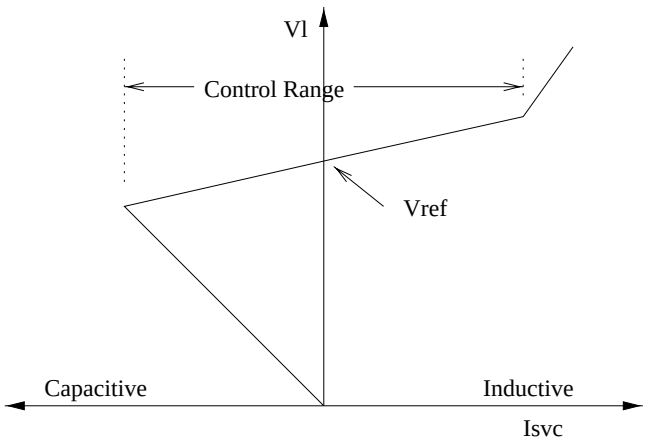

Fig. 4. Typical steady-state voltage control strategy of an SVC.

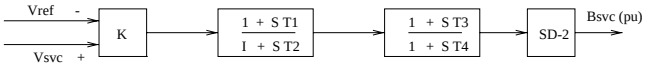

Fig. 5. Block diagram of User Defined SVC used in [18, 19].

In order to determine the most suitable placement of an SVC in the system, a standard voltage collapse technique based on finding the most voltage sensitive bus (the "critical" bus) for the greatest favorable impact on transmission system voltages is used [13]. This technique defines the weakest bus as the one with the largest voltage magnitude entry on the "tangent" vector at or near the voltage collapse point (the tip of the "PV" or "nose" curve) [14]. It has been shown in [13, 14] that this placement technique results in optimal SVC controller locations to improve voltage profiles, improving at the same time stability margins by increasing the "distance" to a voltage collapse point [20]. However, this might not necessarily result in the best controller placement from the point of view of improving oscillation damping. Since using the same concept of participation factors used for the PSS did not generate adequate locations for the SVC controller, alternative placement methodologies are currently under investigation for improving both voltage profiles and oscillation damping.

IV. Test Example

The test system is an approximated model of an actual power network presented in [12], and consists of 3 generators with AVRs (the AVR data for these units was extracted from [21]), 7 transformers, 16 buses and 9 branches; all loads in the system are modeled as constant power loads for power flow studies and constant impedance loads during dynamic analyses. The one-line diagram of this sample system is shown in Fig. 6.

The steady state equilibrium points at various loading conditions were derived from PFLOW [22]. Eigenvalue analysis and time domain simulation were carried out using MASS [18] and ETMSP [19], respectively. All these packages have the capability of adequately modeling SVC controllers.

The results presented here correspond to the following

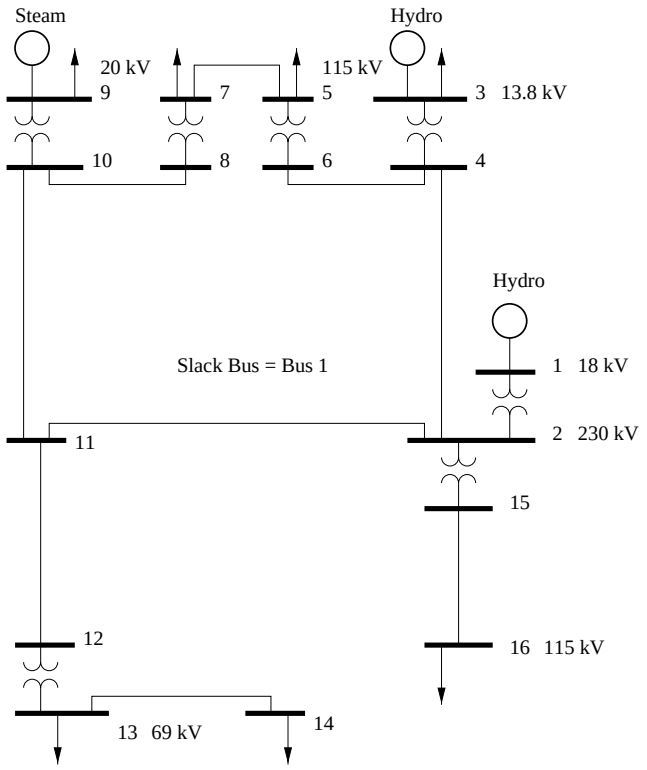

Fig. 6. One-line diagram of test system [12].

studies:

1. Bifurcation and time domain studies of the basic test system, especially to analyze Hopf bifurcations.
2. A PSS controller design to eliminate the Hopf bifurcations.
3. An SVC controller design to eliminate the Hopf bifurcations.

A. *Base System Studies*

The results of these studies are summarized in Fig. 7, which depicts the voltage magnitude at a given load bus versus load changes represented by the following p.u. active power and reactive changes at all load buses:

$$\begin{aligned} P_l &= P_{l_o}(1+\lambda\,\Delta P_l) \\ Q_l &= Q_{l_o}(1+\lambda\,\Delta Q_l) \end{aligned}$$

where the parameter λ, which corresponds to the loading factor (L.F.), represents the slow varying parameter used in bifurcation studies; P_{l_o} and Q_{l_o} stand for the base system load at bus l; and ΔP_l and ΔQ_l represent a fixed direction of loading increase (constant power factor for this example).

Based on the eigenvalue analysis, the solid line in Fig. 7 represents stable equilibrium points, whereas the dashed line is used to depict unstable equilibrium points. At a L.F. of approximately 0.24 p.u., a Hopf bifurcation condition is detected, i.e., the eigenvalues cross over the imaginary axis from the left-half plane to the right-half plane as the L.F. is increased; the most relevant eigenvalues corresponding to this loading condition are depicted in Fig. 8. The maximum loading point on Fig. 7 correspond to a saddle-node

TABLE I
PARTICIPATION FACTORS AT HOPF BIFURCATION

State	Part. Fact.	State	Part. Fact.	State	Part. Fact.
ω_{r1}	0.051	ω_{r2}	0.006	ω_{r3}	0.024
δ_1	0.054	δ_2	0.003	δ_3	0.047
Ψ_{Fd1}	0.003	Ψ_{Fd2}	0.013	Ψ_{Fd3}	1.000
T_{F1}	0.001	T_{F2}	0.012	T_{F3}	0.939
T_{A1}	0.000	T_{A2}	0.000	T_{A3}	0.011
T_{E1}	0.000	T_{E2}	0.001	T_{E3}	0.091

bifurcation point, i.e., a real eigenvalue becomes zero at that point.

An approximate time domain analysis using ETMSP is used to study the behavior of various system variables near the Hopf bifurcation point. The system is assumed to be operating near the Hopf bifurcation condition, i.e., at a L.F. slightly less than 0.24. p.u., when the load at bus 16 is suddenly increased by 3% to simulate a small contingency in the system. The results of this simulation are depicted on Fig. 9; observe the sustained oscillations in all generator frequencies due to a Hopf bifurcation, as expected. (The frequencies do not oscillate about 60 Hz, as automatic control of generators active powers in response to load changes are not modeled in this case.)

B. PSS Design

In order to find out the best location for the PSS, a participation factor analysis was carried out, as described in Section III; this yields the state variables more closely associated with the Hopf bifurcation critical eigenvalues. The magnitudes of the normalized participation factors at the Hopf bifurcation are given in Table I.

It is clear from Table I that T_{F3} and Ψ_{Fd3}, which are state variables that belong to generator 3, are the most dominant at the Hopf bifurcation condition. Based on these results, generator 3 was selected for the placement of the PSS. Typical parameter values for PSS were selected from reference [21] based on generator ratings.

The results of adding the PSS to the system are depicted in Figs. 10 and 11, which show that the Hopf bifurcation has been removed and the system is able to reach the maximum loading conditions. Notice, however, that there is no change in the maximum value of the L.F., which is not the case when the SVC is introduced, as discussed below.

A sensitivity study of the effect of the PSS gain on the critical eigenvalue (the one closer to the imaginary axis) was carried out. Fig. 12 shows that the gain of the PSS has a large effect on the steady-state stability of the system. Hence, the gain should be adjusted with great care to avoid making the system unstable, as the critical eigenvalue crosses the imaginary axis for some values of the PSS gain.

Finally, time domain simulations are carried out for the same small contingency of a 3% load increase at bus 16 as before. The system with PSS (400 gain) is assumed to be loaded at a L.F. value near 0.24 p.u., i.e., at a loading condition close to where the Hopf bifurcation was previously found. Fig. 13 indicates that the PSS rapidly damps the system oscillations, as expected.

C. SVC Design

Simulations are now carried out with an SVC located at bus 13, which is the weakest bus of the system (determined

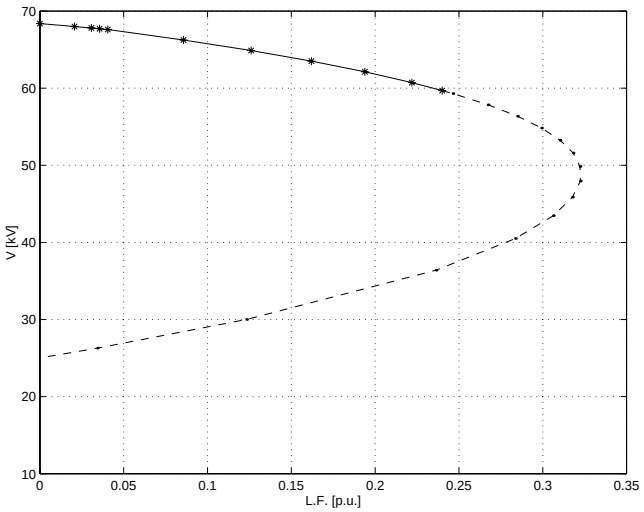

Fig. 7. Voltage profile at bus 16.

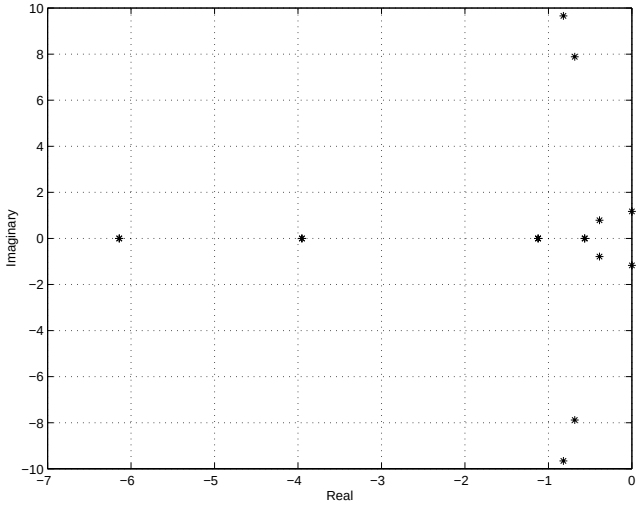

Fig. 8. Plot of a few relevant eigenvalues at the Hopf bifurcation condition.

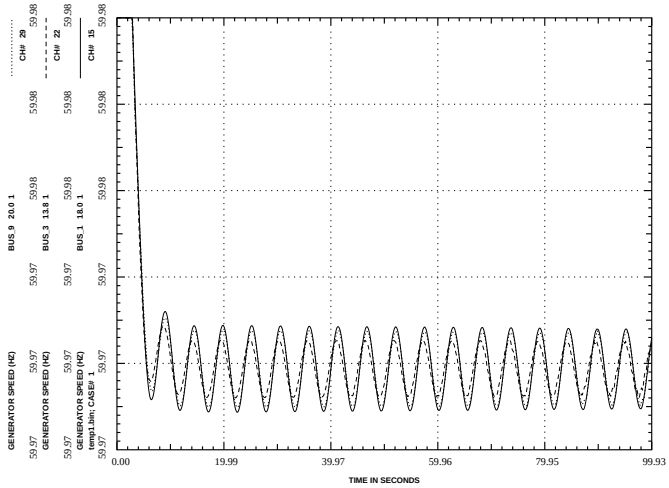

Fig. 9. Generator frequency oscillations due to Hopf bifurcation problem.

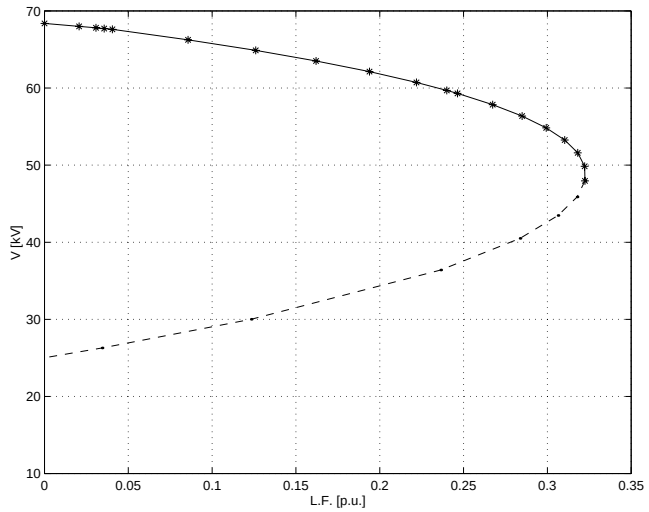

Fig. 10. Voltage profile at bus 16 for system with PSS.

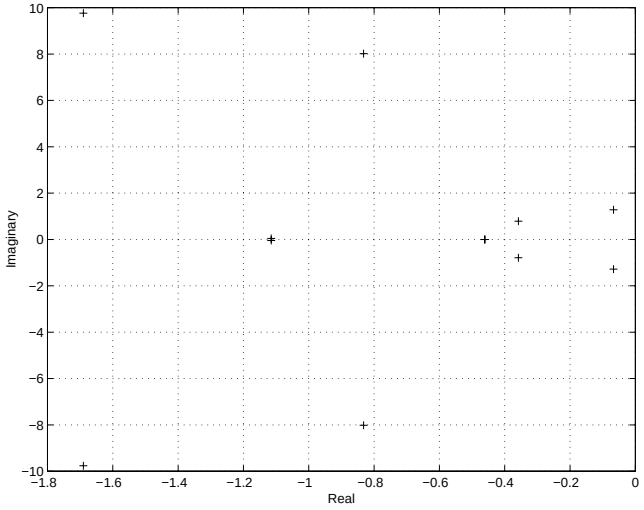

Fig. 11. Plot of a few relevant eigenvalues near the maximum loading conditions for system with PSS

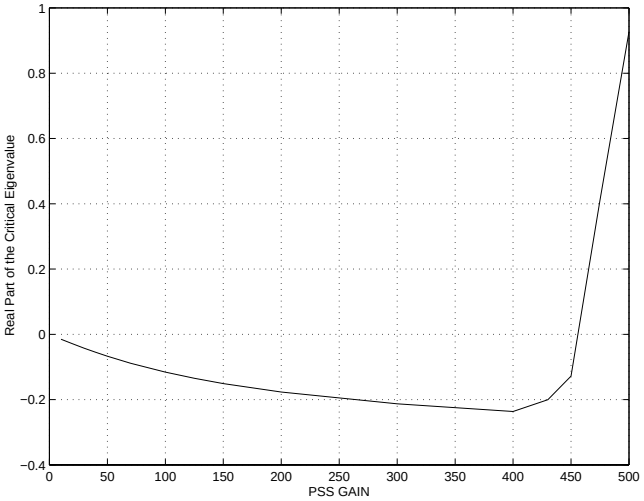

Fig. 12. Critical eigenvalue versus PSS gain.

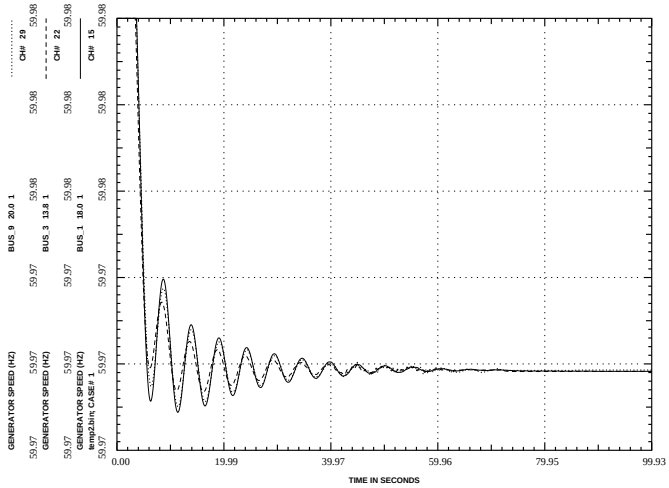

Fig. 13. Generator frequency oscillations for system with PSS.

using the tangent vector technique previously described). The SVC is assumed to have ± 100 Mvar reactive power limits. (Various techniques are proposed in [13] to choose appropriate SVC ratings based on voltage collapse studies.)

As shown in Figs. 14 and 15, the SVC also removes the Hopf bifurcation. However, its effect on system damping is much smaller than that of the PSS, as demonstrated by the very low sensitivity of the critical eigenvalue to the SVC gain depicted in Fig. 16, and the low damping effect on oscillations illustrated in the time domain plots of Fig. 17. On the other hand, the maximum L.F. value has significantly increased from about 0.32 to approximately 0.4 p.u.

V. Conclusions

This paper demonstrates the direct association between typical power/frequency oscillations in power systems and Hopf bifurcations, so that bifurcation theory can be used to design remedial measures to resolve oscillation problems. Furthermore, the paper shows that these Hopf bifurcations can be either controlled at the generator side by using PSS controllers, or in the transmission system by using SVC controllers.

As would expected, the results indicate that PSS controllers are more effective removing oscillations than SVCs. These results, however, are preliminary, since they were obtained using standard SVC voltage controls and placement techniques more appropriate for improving voltage stability. Hence, several studies are currently under way to determine the location techniques, control signals and types of FACTS controllers for optimally damping these oscillations.

References

[1] P. Kundur, *Power System Stability and Control*, McGraw Hill, New York, 1994.

[2] M. J. Lautenberg, M. A. Pai and K. R. Padiyar, "Hopf Bifurcation Control in Power System with Static Var Compensators," *Int. J. Electric Power and Energy Systems*, 1997, Vol. 19, No. 5, pp. 339–347.

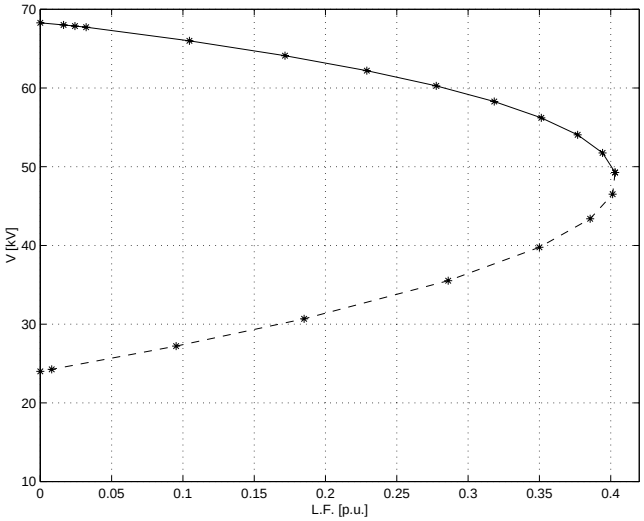

Fig. 14. Voltage profile at bus 16 for system with SVC.

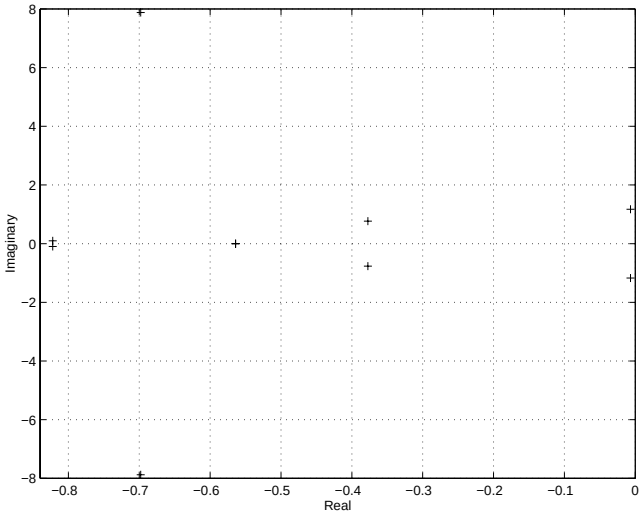

Fig. 15. Plot of a few relevant eigenvalues near the maximum loading conditions for system with SVC

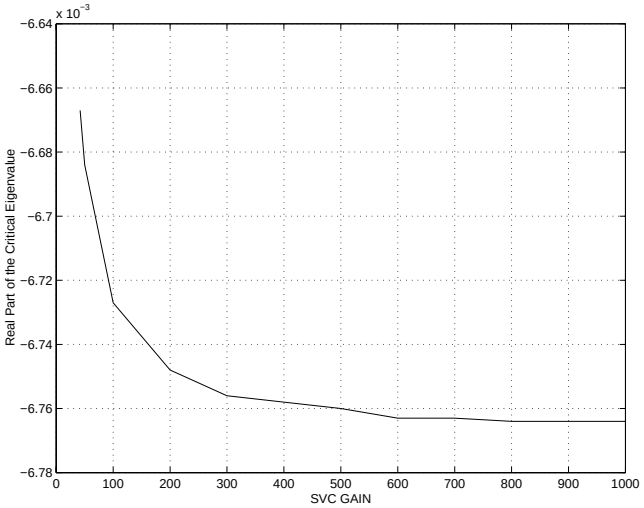

Fig. 16. Critical eigenvalue versus SVC gain.

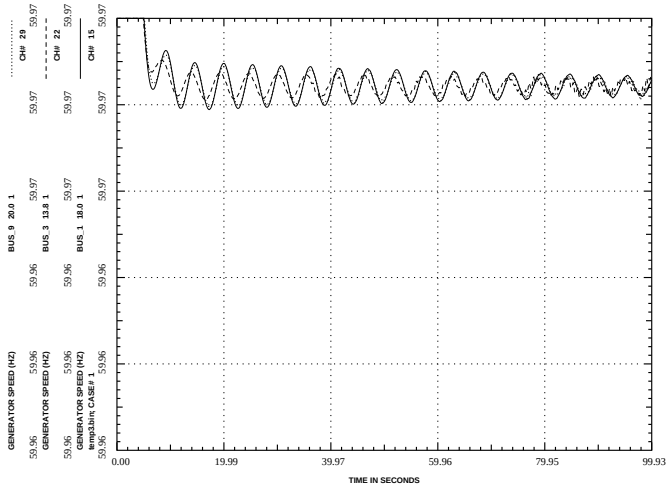

Fig. 17. Generator frequency oscillations for system with SVC.

[3] N. G. Hingorani, "Flexible AC Transmission Systems," *IEEE Spectrum*, pp. 40–45, Apr. 1993.

[4] K. R. Padiyar, and A. M. Kulkarni, "Control Design and Simulation of Unified Power Flow Controller," *IEEE Trans. Power Delivery*, Vol. 13, No. 4, pp. 1348–1354, Oct. 1998.

[5] C. A. Cañizares, F. L. Alvarado, C. L. DeMarco, I. Dobson and W. F. Long, "Point of Collapse Methods Applied to AC/DC Power Systems," *IEEE Trans. Power Systems*, Vol. 7, No. 2, May 1992, pp. 673–683.

[6] P. Kundur, Editor, "Voltage Stability Assessment, Procedures and Guides," IEEE/PES Power Systems Stability Subcommittee, Draft, July 1999. Available at http://www.power.uwaterloo.ca.

[7] V. Ajjarapu and B. Lee, "Bifurcation Theory and its Application to Nonlinear Dynamical Phenomena in Power System," *IEEE Trans. Power Systems*, Vol. 7, No. 2, pp. 424–431, Feb. 1992.

[8] E. H. Abed and P. P. Varaiya, "Nonlinear Oscillation in Power Systems," *Int. J. Electric Power and Energy Systems*, Vol. 6, pp. 37–43, 1984.

[9] C. A. Cañizares and S. Hranilovic, "Transcritical and Hopf Bifurcations in AC/DC Systems," *Proc. Bulk Power System Voltage Phenomena III—Voltage Stability and Security*, Davos, Switzerland, pp. 105–114, Aug. 1994.

[10] C. A. Cañizares, "On Bifurcation, Voltage Collapse and Load Modelling," *IEEE Trans. Power Systems*, Vol. 10, No. 1, pp. 512–522, Feb. 1995.

[11] N. Mithulananthan and S. C. Srivastava, "Investigation of a Voltage Collapse Incident in Sri Lanka's Power System Network," *Proc. of EMPD'98, Singapore*, IEEE Catalogue No. 98EX137, pp. 47–52, Mar. 3-5, 1998.

[12] C. A. Gross, *Power System Analysis*, Second Edition, John Wiley & Sons, 1986.

[13] C. A. Cañizares and Z. T. Faur, "Analysis of SVC and TCSC Controllers in Voltage Collapse," *IEEE Trans. Power Systems*, Vol. 14, No. 1, pp. 158–165, Feb. 1999.

[14] C. A. Cañizares, A. Berizzi, and P. Marannino, "Using FACTS Controllers to Maximize Available Transfer Capability," *Proc. Bulk Power Systems Dynamics and Control IV–Restructuring*, Santorini, Greece, 633-641, Aug. 1998.

[15] R. Seydel, *Practical Bifurcation and Stability Analysis: From Equilibrium to Chaos*, Second Edition, Springer-Verlag, New York, 1994.

[16] D. J. Hill and I. M. Y. Mareels, "Stability Theory for Differential/Algebraic Systems with Application to Power Systems," *IEEE Trans. Circuits and Systems*, Vol. 37, No. 11, pp. 1416–1423, Nov. 1990.

[17] L. Gyugyi, "Power Electronics in Electric Utilities: Static Var Compensators," *Proc. IEEE*, Vol. 76, No. 4, pp. 483–494, Apr. 1988.

[18] "Small Signal Stability Analysis Program Ver. 3.1: User's Manual," EPRI, TR-101850-V2R1, May 1994.

[19] "Extended Transient-Midterm Stability Program (ETMSP) Ver. 3.1: User's Manual," EPRI, TR-102004-V2R1, May 1994.

[20] C. A. Cañizares, "Calculating Optimal System Parameters to Maximize the Distance to Saddle-node Bifurcations," *IEEE Trans. Circuits and Systems–I*, Vol. 45, No. 3, pp. 225–237, Mar. 1998.

[21] P. M. Anderson and A. A. Fouad, *Power System Control and Stability*, IEEE Press, 1994.

[22] C. A. Cañizares, et. al, "PFLOW: Continuation and Direct Methods to Locate Fold Bifurcations in AC/DC/FACTS Power Systems," University of Waterloo, August 1998. Available at http://www.power.uwaterloo.ca.

Nadarajah Mithulananthan was born in Sri Lanka. He received his B.Sc. (Eng.) and M.Eng. degrees from the University of Peradeniya, Sri Lanka, and the Asian Institute of Technology, Thailand, in May 1993 and August 1997, respectively. Mr. Mithulananthan has worked as an Electrical Engineer at the Generation Planning Branch of the Ceylon Electricity Board, and as a Researcher at Chulalongkorn University, Thailand. He is currently a full time Ph.D. student at the University of Waterloo working on applications and control design of FACTS controllers.

Claudio A. Cañizares received in April 1984 the Electrical Engineer diploma from the Escuela Politécnica Nacional (EPN), Quito-Ecuador, where he held different teaching and administrative positions from 1983 to 1993. His M.Sc. (1988) and Ph.D. (1991) degrees in Electrical Engineering are from the University of Wisconsin–Madison. Dr. Cañizares is currently an Associate Professor at the University of Waterloo, E&CE Department, and his research activities are mostly concentrated in studying stability, modeling and computational issues in ac/dc/FACTS systems.

John Reeve received the B.Sc., M.Sc., Ph.D. and D.Sc. degrees from the University of Manchester (UMIST). After employment in the development of protective relays for English Electric, Stafford, between 1958 and 1961, he was a lecturer at UMIST until joining the University of Waterloo in 1967, where he is currently an Adjunct Professor in the Department of Electrical & Computer Engineering. He was a project manager at EPRI, 1980-81, and was with IREQ, 1989-1990. His research interests since 1961 have been HVDC transmission and high power electronics. He is the President of John Reeve Consultants Limited. Dr. Reeve was chair of the IEEE DC Transmission Subcommittee for 8 years, and is a member of several IEEE and CIGRE Committees on dc transmission and FACTS. He was awarded the IEEE Uno Lamm High Voltage Direct Current Award in 1996.